JOURNAL OF MATERIALS SCIENCE 33 (1998) 3345–3350

Effect of BTA on electrochemical corrosion and stress corrosion cracking behaviour of type 304 stainless steel in 1 M HCl

A. DEVASENAPATHI*, V. S. RAJA
Corrosion Science and Engineering Program, Indian Institute of Technology (Bombay), Mumbai 400 076, India
E-mail: vsraja@cc.iitb.ernet.in

Effect of benzotriazole (BTA) on polarization and stress corrosion cracking (SCC) behaviour of type 304 stainless steel in 1 M HCl was investigated. The anodic polarization curves showed that with BTA additions the anodic polarization kinetics in the active region was not affected, though a reduction in critical current density, i_{crit}, and passive current density, i_p, was observed. However, BTA was found to influence significantly the cathodic reaction kinetics. SCC results using smooth tensile test specimens showed an increase in time-to-failure, t_f, with BTA additions. Crack growth rate studies using single-edge notched (SEN) specimens showed an increase in threshold stress intensity for SCC, K_{ISCC}, and a decrease in crack growth rate, da/dt, with BTA additions. While the adsorption isotherms derived from weight loss data followed a Langmuir adsorption isotherm signifying a monolayer adsorption, the adsorption isotherms derived from SCC test data deviated from this at higher BTA concentrations. The paper discusses the possible reason for this deviation.

1. Introduction

Benzotriazole (BTA) has long been known as an effective inhibitor for copper and copper alloys [1, 2]. Though its effect on ferrous alloys has not been widely studied, it is reported to provide inhibition for iron [3–7], mild steel [8–10] and Fe–Ni alloys against corrosion in mineral acids. The inhibiting effect of BTA in reducing the hydrogen absorption tendency in iron and mild steel [5, 6, 8] has also been reported. Studies on iron [3–7], Fe–Ni alloys [11] show that BTA inhibits hydrogen evolution kinetics by adsorbing on the active sites. While most of the studies have been reported on the inhibitive action of BTA on iron, mild steel and HSLA steels, its influence on corrosion and hydrogen evolution reactions on stainless steels is not well studied. Studies carried out [12] on 410 stainless steel show that BTA reduces the cathodic hydrogen evolution reaction and also decreases the hydrogen embrittlement behaviour of these stainless steels under cathodic charging conditions. While most of the studies indicate the role of BTA to be to reduce the cathodic hydrogen evolution reaction and consequently corrosion rate, its influence on the anodic polarization behaviour of an active passive alloy has not been studied. Furthermore, several studies have been carried out on the SCC behaviour of type 304 stainless steel in acidic solution. However, barring a few studies [13], the role of BTA as an inhibitor against SCC is not well studied. Thus the present study is aimed to understand the role of BTA towards electrochemical corrosion and SCC of an active-passive alloy, namely type 304 stainless steel.

2. Experimental procedure

The composition of type 304 stainless steel in wt% used in this study was 0.04C, 0.71Si, 1.72Mn, 8.5Ni, 18.8Cr, 0.12Cu, 0.046P, 0.017N and 0.019S. The specimens of required dimensions were machined from the alloy and used after solution-treated at 1075 °C in a nitrogen atmosphere for 1 h, followed by water quenching. Experiments were conducted with specimens wet-ground to 600 grit finish using silicon carbide paper, followed by mirror polishing using wet alumina. Four different experiments (weight loss, potentiodynamic polarization, constant load SCC tests using smooth tensile test specimens and crack growth studies using single-edge notch (SEN) specimens) were carried out. The test solution used was 1 M HCl at room temperature exposed to air. The effect of BTA addition on weight loss, potentiodynamic polarization and SCC was studied in five different concentration ranges starting from 1×10^{-3} to 1×10^{-1} M. The test solutions were prepared using AnalaR grade chemicals of HCl and BTA in distilled water.

* *Present Address*: Department of Mechanical Systems Engineering, Faculty of Engineering, Shinshu University, Nagano - 380, Japan.

Weight-loss experiments were performed using specimens of dimension 50 mm × 50 mm × 0.6 mm in triplicate. The tests were conducted for 240 h by placing them into the test solution. After the stipulated time period, samples were taken out rinsed with distilled water, dried and weighed for change in weight from its initial weight.

For polarization studies, specimens of 1 cm^2 area cold set in polyacrylic powder were used. Potentiodynamic polarization studies were carried out using a PARC Model 273 potentiostat operated with m352 software at a scan rate of 1 $mV\,s^{-1}$ using platinum as a counter electrode and a saturated calomel as the reference electrode.

For time-to-failure SCC tests, smooth flat tensile test specimens of 25 mm gauge length, 6 mm width machined from strips of 100 mm length giving a reduced length of 40 mm, were used. All the specimens were tested at 75% of their yield strength, which was 22.5 $kg\,mm^{-2}$, in a spring loaded constant load SCC testing apparatus at open circuit potential (OCP) [14]. The time to fracture the specimen completely was taken as time to failure.

For crack growth rate studies, SEN specimens of 100 mm length, 25 mm width and 0.6 mm thickness were used. A notch of 8 mm length and 0.4 mm width was made at one edge in the centre with the help of a silicon carbide wheel. The crack growth rate studies were carried out in a spring-loaded constant load SCC test apparatus. The details of the spring-loaded SCC test apparatus are described elsewhere [15]. The crack growth rates, da/dt, were obtained by measuring the initial crack length and change in the crack length with time using a travelling microscope with the help of a light source. Stress intensity calculations were made as described by Singh and Altstetter [16].

In order to ascertain the threshold stress intensity of SCC, K_{ISCC}, the SEN specimens were loaded at different stress intensity values and exposed to the test environment. The alloy was considered resistant to SCC at those stress intensity values which resulted in crack growth rates lower than $10^{-10}\,m\,s^{-1}$. The lowest stress intensity value at which the crack propagation rate was $10^{-10}\,m\,s^{-1}$ and above, was taken as the K_{1SCC}. The specimens were loaded at these K_{1SCC} values for crack growth rate studies. As the crack grows, the stress intensity, $K1$, at the crack tip increases. So the crack tip is subjected to different stress intensity levels without altering the applied load. Hence, during the course of the experiment with the progress in crack growth, a net increase in stress intensity is always observed. The spring relaxation associated with crack growth was measured using a dial gauge to determine the extent of relaxation and the subsequent decrease in the applied load. It is necessary to emphasize the fact that this decrease in applied load lowers the stress intensity only to a lesser extent than the stress intensity increase caused by the crack growth. During crack growth experiments, the formation of microcracks ahead of the main crack, and the joining of both with the growth of a main crack, was also observed. The failed specimens were ultrasonically cleaned in 1 M HCl, washed with distilled water followed by methanol. The specimens were dried in hot air and analysed for fracture morphology in a scanning electron microscope (SEM).

3. Results and discussion

3.1. Weight loss

The weight loss data show that the increase in BTA concentration, the corrosion rate is lowered. Because BTA provides protection by adsorbing on the alloy surface, its efficiency is related to the total coverage it provides to the alloy [1]. The coverage for various concentrations of inhibitors were calculated from the relation

$$(1 - W/W_0) \times 100 \qquad (1)$$

where W_0 and W are the weight losses without and with inhibitor, respectively. An adsorption isotherm curve fitted using the log–log plots of total concentration versus coverage, is shown in Fig. 1. The plot shows a slope of unity obeying a Langmuir adsorption isotherm. As Langmuir isotherm signifies the monolayer adsorption behaviour of molecules on the alloy surface, shows that BTA inhibits corrosion by monoplayer adsorption on the alloy surface. Similar adsorption behaviour which follows a Langmuir adsorption isotherm has been reported for the inhibition of copper by BTA [1].

3.2. Potentiodynamic polarization

Potentiodynamic polarization results of type 304 stainless steel without and with varying concentrations of BTA are given in Fig. 2. Electrochemical kinetic parameters derived from these experiments are given in Table I. Owing to the uncertainty in the anodic Tafel region, i_{corr} was not derived from these curves. The table shows that with the addition of BTA, the open circuit potential (OCP) is shifted towards a more noble direction. The initial addition of BTA to the extent of 1×10^{-3} M results in a significant shift of 100 mV in the noble direction. A subsequent increase in BTA concentration influences OCP only marginally. Examination of cathodic curves shows that the cathodic reaction is reduced with the addition of BTA, as it is shifted towards lower current density values while bringing no significant change in the cathodic Tafel slope. This shows that BTA brings down the cathodic hydrogen evolution reaction without modifying the mechanism of hydrogen evolution reaction in an uninhibited solution. Such an effect is possible due to the reduction in electrode surface available for hydrogen evolution reaction by BTA coverage. A similar effect of BTA on the cathodic hydrogen evolution mechanism has been reported [12] for 410 stainless steel in 0.5 M H_2SO_4.

In sharp contrast to cathodic polarization curves, the anodic polarization curves show that BTA additions increase the anodic dissolution behaviour of the alloy in the active region. This is exhibited by the slight reduction in the slope of the curves till the critical current density, i_{crit} is reached. The effect of BTA on i_{crit} and passive current density, i_p, are

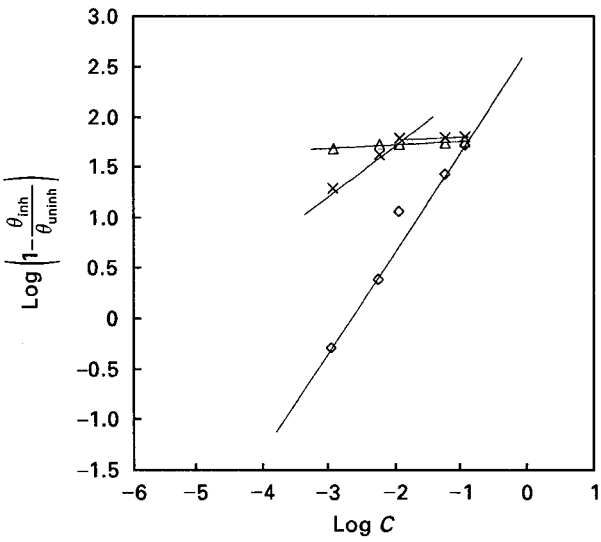

Figure 1 Typical absorption isotherms derived from (◇) weight loss, (x) time to failure, and (△) K_{ISCC} data.

summarized in Table I. The i_{crit} is reduced to a large extent by BTA, which is exhibited by the reduction in the nose of the active passive transition curve towards lower current density values. Also, i_p is reduced, though there is no change in the potential range of passivation. The lowering of the i_{crit} and i_p values by the BTA additions show that BTA exerts some influence in stabilizing the passive film, though the passive potential region is not modified. This is indicated by the following observations; (i) the active anodic dissolution is not reduced until i_{crit} is reached; (ii) i_{crit} and i_p are reduced; (iii) above 0.1 V the inhibition efficiency is lost as exhibited by an irregular increase in the transpassive dissolution of the alloy.

TABLE I Electrochemical parameters derived from the polarization experiments carried out in 1 M HCl

Environment	OCP (V) versus SCE	i_{crit} (mA cm^{-2})	i_p (mA cm^{-2})	β_c (mV/decade)
Without inhibitor	−0.440	9.55	1.37	91
1×10^{-3} M	−0.334	4.55	0.94	105
5×10^{-3} M	−0.322	3.475	0.90	106
1×10^{-2} M	−0.311	3.236	0.765	110
5×10^{-2} M	−0.300	2.12	0.52	114
1×10^{-1} M	−0.268	1.61	0.347	121

TABLE II SCC test results of type 304 stainless steel in 1 M HCl with and without BTA

Environment	Time to failure (h)
1 M HCl	57
1 M HCl + 1×10^{-3} M BTA	74
1 M HCl + 5×10^{-3} M BTA	137
1 M HCl + 1×10^{-2} M BTA	157
1 M HCl + 5×10^{-2} M BTA	184
1 M HCl + 1×10^{-1} M BTA	223

3.3. Stress corrosion cracking (SCC)

3.3.1. Time to failure

The effect of BTA towards SCC of type 304 stainless steel in 1 M HCl is given in Table II. With the increase in BTA concentration, the time to failure increases, indicating that BTA promotes SCC resistance of stainless steels in 1 M HCl. Fractographic studies carried out using SEM showed a transgranular mode of cracking (TG) both in 1 M HCl and in solutions with BTA additions.

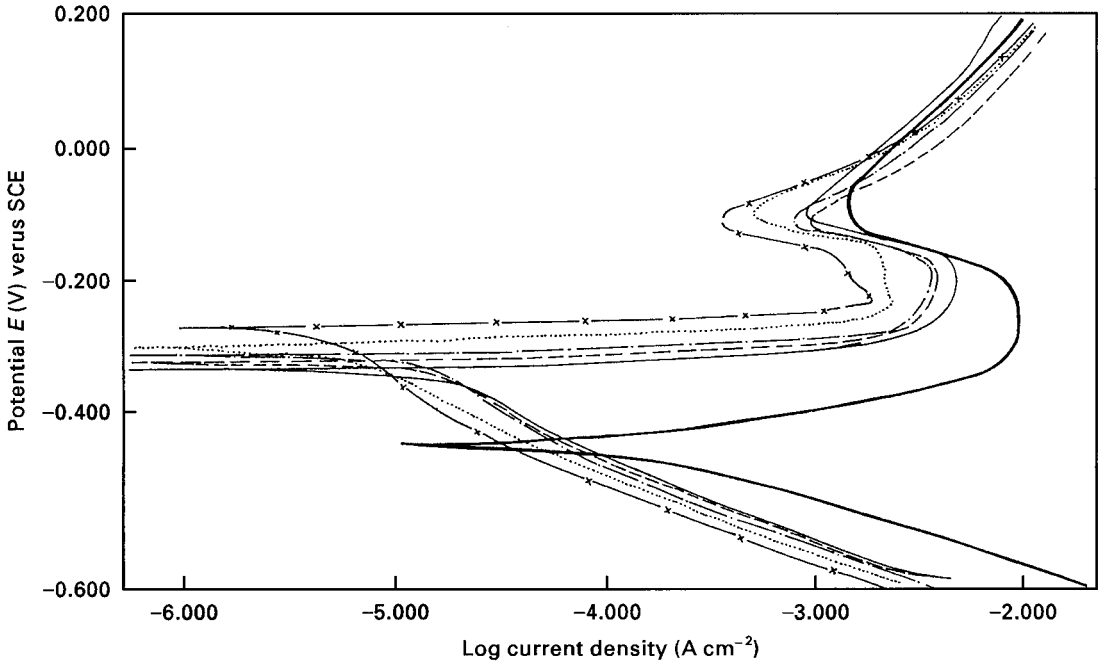

Figure 2 Potentiodynamic polarization behaviour of AISI 304 stainless steel in (———) 1 M HCl and with (———) 1×10^{-3} M, (- - -) 5×10^{-3} M, (—x—) 1×10^{-2} M, (···) 5×10^{-2} M and (—x—) 1×10^{-1} M BTA additions.

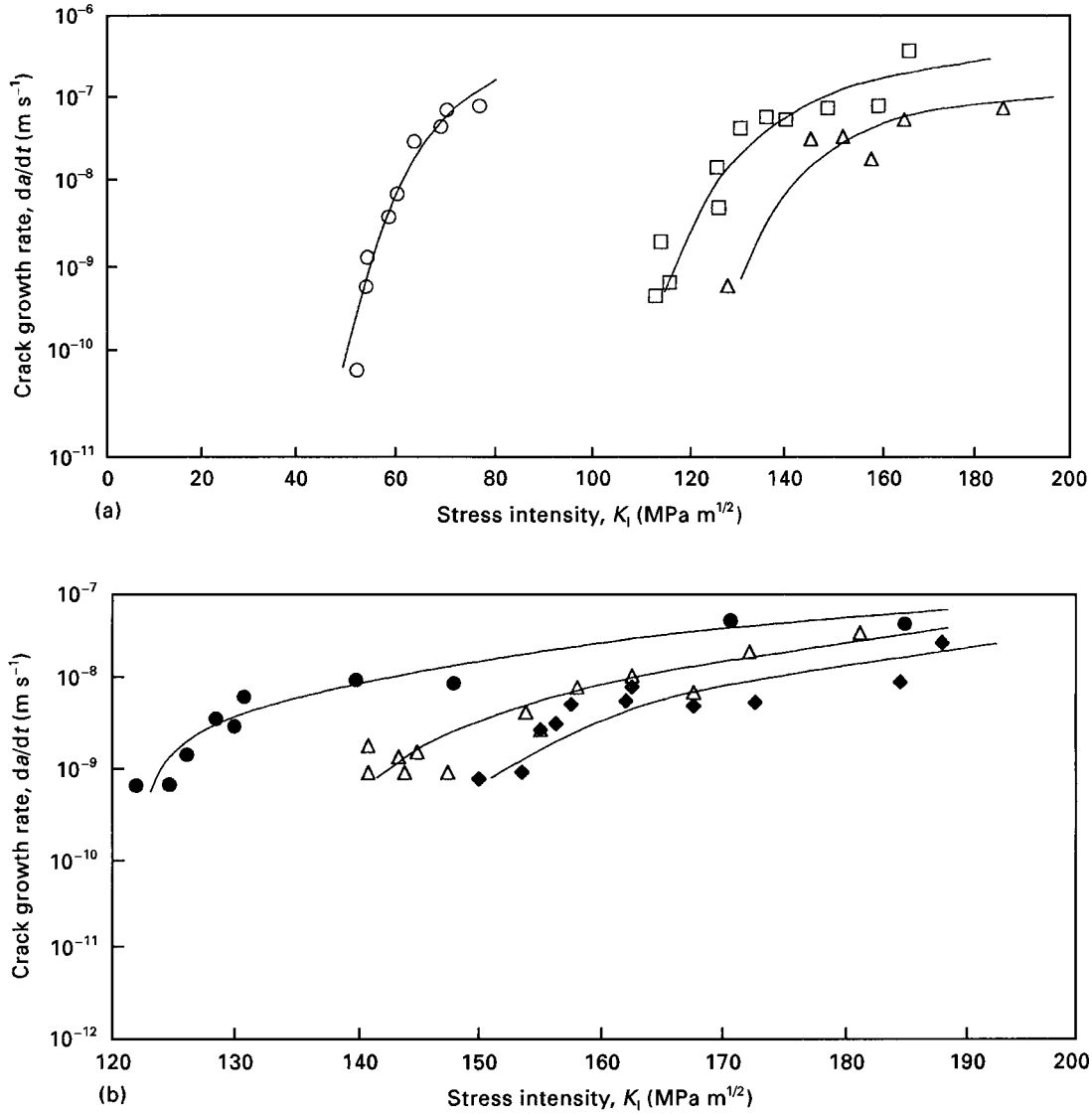

Figure 3 Crack growth behaviour of type 304 stainless steel in (○) 1 M HCl and with (a) (□) 1×10^{-3} M and (△) 5×10^{-3} M BTA additions, and (b) (●) 1×10^{-2} M, (△) 5×10^{-2} M and (◆) 5×10^{-1} M BTA additions.

3.3.2. Crack growth rates

The crack growth rate, da/dt, versus stress intensity $K1$, curves obtained for type 304 stainless steel in 1 M HCl and with BTA additions, are shown in Fig. 3a and b. The parameters derived from the crack growth rate experiments are given in Table III. $K1$SCC for type 304 stainless steel in 1 M HCl was found to be 52 MPa m$^{1/2}$ which was lower than the plane stress fracture toughness of 240 MPa m$^{1/2}$ observed in air. With the addition of 10^{-3} M BTA, the value of $K1$SCC increased to 113 MPa m$^{1/2}$. BTA additions at higher concentrations led to a further increase in $K1$SCC values as shown in Fig. 3a and b. This increase in $K1$SCC values with BTA additions showed that a higher incubation time was needed at lower stress intensity values for the crack to propagate [17]. So the stress intensity was increased to attain a crack growth rate of 10^{-10} m s^{-1}. Further, in 1 M HCl the (da/dt) versus $K1$ curve showed an increase in crack growth with increase in stress intensity, $K1$ (Fig. 3a). In this case no stage II slow crack growth behaviour was observed. On the contrary, with BTA additions, a clear stage II slow crack growth behaviour was noticed (Fig. 3a and b). In addition, the crack growth rates significantly decreased with BTA additions. It should be noted that while the alloy showed a maximum crack growth rate of 1×10^{-7} m s^{-1} at a stress intensity value of 80 MPa m$^{1/2}$ in 1 M HCl, the addition of 1×10^{-1} M BTA reduced the crack growth rate to 1×10^{-8} m s^{-1} even at a higher stress intensity value of 175 MPa m$^{1/2}$.

It is well known that at low stress intensity $K1$ values, da/dt is strongly dependent on $K1$ (stage I); at intermediate values of $K1$ (stage II), da/dt becomes relatively independent of $K1$ and as $K1$ approaches the critical value of stress intensity K_c, da/dt increases rapidly (stage III). On the contrary, the rapid rise in crack growth rate da/dt in 1 M HCl at stage I and the absence of a slow crack growth stage (stage II), indicate that the alloy underwent a fast fracture due to the high anodic dissolution at the crack tip as well by the hydrogen absorption into the alloy. Previous studies also indicated that in certain alloy–environment combinations, stage II may be missing due to fast fracture at the start of stage II [18]. With BTA additions, stage II occurred at the higher $K1$ values of around 140 MPa m$^{1/2}$.

TABLE III Change in K_{ISCC} values with BTA additions

Environment	K_{ISCC}(MPa m$^{1/2}$)
In air	240 (K_c)
1 M HCl	52
1 M HCl + 1×10^{-3} M BTA	113
1 M HCl + 5×10^{-3} M BTA	120
1 M HCl + 1×10^{-2} M BTA	124
1 M HCl + 5×10^{-2} M BTA	141
1 M HCl + 1×10^{-1} M BTA	150

In order to understand the nature of inhibition with respect to SCC, adsorption isotherms were drawn based on time to failure and K1SCC data. In the case of type 304 stainless steel, the behaviour towards time to failure per cent inhibition of SCC was obtained using the relation

$$\% \text{ SCC inhibition} = (1 - t_0/t_i) \times 100 \quad (2)$$

while in the case of alloy response to crack growth, the per cent inhibition was calculated using the relation

$$\% \text{ SCC inhibition} = (1 - K1SCC_{(0)}/K1SCC_{(i)} \times 100 \quad (3)$$

both these relationships are similar to that applied for uniform corrosion, as given in Equation 1. In the above equations, t_0 and t_i represent the time to failure of specimens without and with inhibitor addition and $K1SCC_{(0)}/K1SCC_{(i)}$ represent the threshold stress intensity for crack growth without and with the addition of inhibitors, respectively. Use of the time to failure and the K_{ISSC} data to calculate the inhibition efficiency was justified for the following reasons. These stainless steels are proposed to undergo SCC by an active path anodic dissolution process. In this case, the crack growth is directly proportional to the anodic current density, i_a, at the crack tip through the following relation [19].

$$\text{crack velocity, } da/dt = i_a M/zF\rho \quad (4)$$

where M is the atomic weight of the metal, z is the valency of the metallic ion, F is the Faraday constant and ρ is density. Because the anodic current density can be affected by the adsorption of inhibitors, the lowering of i_a due to the addition of inhibitor and the consequent rise in time to failure and K1SCC, can be related to the nature of adsorption of the inhibitors.

Though there have been few studies on the effect of inhibitors on SCC behaviour [12], these studies did not examine the data in the light of the adsorption isotherm. The present study attempts to correlate the adsorption isotherm to the role of inhibitor towards SSC. The isotherms clearly reflected the following parts.

(a) The isotherm of weight loss data showed a typical Langmuir adsorption isotherm having a slope of unity. On the contrary, the isotherms of time to failure and K1SCC data were quite different (Fig. 1). Isotherms derived from time to failure data showed a slope of 0.5 at lower concentrations of BTA, which decreased to 0.075 at higher concentrations, whereas the isotherm derived from K1SCC data showed a slope of 0.05 at all concentrations of BTA. The decrease in slope observed in the isotherms derived from time to failure and K1SCC data indicated that they did not obey the Langmuir behaviour of adsorption.

(b) Interestingly, the isotherms derived based on time to failure and K_{ISSC} data lay very close to each other, despite the fact that the former involved a smooth sample while the latter involved the precracked samples. In the smooth sample, SCC is expected to occur by nucleation and growth of cracks, while in the precracked samples SCC occurs exclusively due to the crack growth process. The fact that both the adsorption isotherms behaved in a similar manner indicated that BTA inhibitor was effective during the crack growth stage of SCC. The current results reflected this proposition, as discussed below.

The results shown in Tables II and III indicate that the initial addition of BTA (10^{-3} M) had sharply increased the SSC resistance of type 304 stainless steel, while a subsequent addition had only a marginal effect. In this range, the isotherm deviated from Langmuir behaviour. The deviation from Langmuir behaviour was reported normally due to the interaction among the inhibitor molecules [20]. Therefore, the question arises as to why there should be interaction among the adsorbing molecules in the case of 304 type stainless steel subjected to stress, whereas such an interaction did not exist in the case of unstressed sample as shown by the adsorption isotherm corresponding to the weight loss data. In the absence of any viable explanation, it is necessary to examine the nature of inhibition and its preference to specific sites. This can be done based on the polarization behaviour of 304 type stainless steel in the presence of BTA.

As discussed earlier, polarization curves (Fig. 1) indicated that BTA did not affect the anodic areas and the corrosion rate was brought down by controlling the cathodic reaction. This was also reflected in suppressing the hydrogen evolution during the crack growth rate studies. The preferential adsorption behaviour of inhibitors on active or passive sites in providing corrosion inhibition has been discussed in detail in the review by Trabanelli [21]. In a stainless steel undergoing SCC in 1 M HCl, the alloy as a whole was reported [22] to be in an active state. However, due to the variation in stress concentration, the crack tip remains more active and anodic and the crack walls become more cathodic. So a strong couple exists between the two [22]. When BTA was added at low concentration, they are preferentially adsorbed on the crack walls, as they would be more cathodic than the remaining surface and BTA is a cathodic inhibitor. Subsequent additions of BTA are expected to adsorb on the remaining cathodic areas. Because the cathodic nature of crack walls has a stronger influence on the crack growth than that of the remaining surface, the initial addition of BTA promotes a higher resistance towards SCC than the subsequent ones.

The per cent inhibition obtained by BTA from weight loss and SCC data is given in Table IV. This showed the higher percentage of inhibition towards SCC than that of the general uniform corrosion. This might be due to the fact [8] that BTA reduced cathodic hydrogen evolution on the metal surface thereby

TABLE IV Percentage inhibition obtained from weight loss and time to failure data of type 304 stainless steel in 1 M HCl with BTA additions

BTA concentration (M)	Inhibition(%)	
	Weight loss	Time to failure (h)
1×10^{-3}	0.57	22
5×10^{-3}	2.58	58
1×10^{-2}	12.2	64
5×10^{-2}	27.7	69
1×10^{-1}	56	74

reducing the anodic dissolution and also the hydrogen diffusion into the metal. The effectiveness of BTA in inhibiting the hydrogen absorption has been reported [8] for mild steel in 0.5 M H_2SO_4. Further, studies by Agarwal and Namboodhiri [12] on the hydrogen embrittlement of AISI 410 stainless steel under cathodic charging, also showed the inhibitive effect of BTA on hydrogen absorption. The effectiveness of BTA in decreasing the hydrogen absorption and thereby SCC is further understood from the SCC growth rate studies [23] reported for austenitic stainless steels. These studies [23] showed that in simulated crack tip environments the crack growth rates observed were much higher than that calculated from the general corrosion rates. This increased crack growth was attributed to the hydrogen embrittlement in addition to the active anodic dissolution. The hydrogen diffuses into the austenite matrix and increases the SCC susceptibility. So the increased SCC resistance observed by BTA addition towards SCC can be due to its influence in decreasing the cathodic reaction and a consequent reduction in anodic dissolution at the crack tip and the quantity of hydrogen diffused into the alloy.

4. Conclusions

1. Addition of BTA shifted OCP towards the more noble direction with reduction in i_{crit} and i_p values.

2. With the increase in BTA additions, the time to failure and K_{ISSC} values increased and da/dt values decreased.

3. While weight-loss experiments showed that BTA followed a Langmuir adsorption isotherm signifying a monolayer adsorption, the isotherms derived from the time to failure and K_{ISSC} data deviated from linearity.

4. The increased SCC resistance with BTA additions was attributed to a possible decrease in cathodic reaction and a consequent reduction in anodic current density at the crack tip and the quantity of hydrogen diffused into the alloy.

References

1. P. G. FOX, G. LEWIS and P. J. BODEN, *Corros. Sci.* **19** (1979) 457.
2. S. M. MAYANNA and T. H. V. SHETTY, *ibid.* **15** (1975) 627.
3. T. G. NEZNAMOVA and V. P. BARANNIK, *Dokl. Akad. Nauk. Urn. USSR* **11** (1966) 1451.
4. R. J. CHIN and K. NOBE, *Corrosion* **28** (1972) 345.
5. D. L. DULL and K. NOBE, *ibid.* **35** (1979) 535.
6. Y. SAITO and K. NOBE, *ibid.* **36** (1980) 178.
7. R. J. CHIN and K. NOBE, *J. Electrochem. Soc.* **118** (1971) 545.
8. B. S. CHAUDHARI and T. P. RADHAKRISHNAN, in "Proceedings of the Tenth International Congress on Metallic Corrosion", (SAEST, 1989) p. 2327.
9. N. SUBRAMANYAN, S. K. RANGARAJAN, K. BALAKRISHNAN and B. SATHIANANDAM, *Trans. SAEST* **7** (1972) 108.
10. I. SINGH, A. K. LAHIRI and V. A. ALTEKAR, in "Proceedings of the Fifth International Congress on Metallic Corrosion", Tokyo, (NACE, Texas, 1974) p. 570.
11. DAN ALTURA and KEN NOBE, *Corrosion* **32** (1976) 41.
12. R. AGRAWAL and T. K. G. NAMBOODHIRI, *J. App. Electrochem.* **22** (1992) 382.
13. G. TRABANELLI, A. FRIGNANI and F. ZUCCHI, in "Corrosion Inhibition", Proceedings of the International Conference on Corrosion Inhibition, edited by R. H. Hausler (NACE, Texas, 1983) p. 68.
14. A. DEVASENAPATHI and V. S. RAJA, *Corrosion* **52** (1996) 243.
15. A. DEVASENAPATHI, Doctoral Thesis, Indian Institute of Technology, Bombay (1996).
16. S. SINGH and C. ALTSTETTER, *Metall. Trans.* **13A** (1982) 1799.
17. O. V. KUROV, *Corrosion* **49** (1993) 315.
18. HOWARD G. NELSON and DELL P. WILLIAMS, in "Conference Proceedings on Stress Corrosion Cracking and Hydrogen Embrittlement of Iron Base Alloys", edited by R. W. Staehle, J. Hochmann, R. D. McCright and J. E. Slater (NACE, Texas, 1977) p. 390.
19. R. N. PARKINS, *Corros. Sci.* **20** (1980) 147.
20. T. P. HOAR and R. D. HOLLIDAY, *J. Appl. Chem.* **3** (1953) 502.
21. G. TRABANELLI, in "Corrosion Inhibitors, Corrosion Mechanisms", edited by Florian Mansfeld (Marcel Dekker, New York, 1987) p. 150.
22. J. Y. ZUO, B. X. GU and Y. P. LIU, *Corrosion* **47** (1991) 47.
23. Z. FANG, Y. WU, R. ZHU, B. CAO and F. XIAO, *ibid.* **50** (1994) 873.

Received 17 March 1997
and accepted 22 April 1998